

# Novel efficient, high-resolution and structure-preserving convection schemes for computational fluid dynamics

Xi Deng, Zhen-hua Jiang, Omar Matar

Department of Chemical Engineering, Imperial College London, United Kingdom

77th Annual Meeting of the Division of Fluid Dynamics

# Contents

## 1 Introduction

- Research Background
- Research Aim

## 2 A Unified Framework for Non-linear Schemes in a Compact Stencil

- Definitions and Properties of the Normalised Variable
- Accuracy Condition
- Review of Existing Non-linear Schemes
- Unified Normalised-variable Diagram

## 3 Reconstruction Operator on Unified Normalised-variable Diagram (ROUND) schemes

## 4 Extension to unstructured girds and implementation into OpenFoam

## 5 Conclusion

# Research Background

1D conservation law

$$\frac{\partial \phi}{\partial t} + \frac{\partial f(\phi)}{\partial x} = 0, \quad (1)$$

Finite volume method

$$\frac{d\bar{\phi}_i}{dt} = -\frac{1}{h}(\tilde{f}_{i+\frac{1}{2}} - \tilde{f}_{i-\frac{1}{2}}), \quad (2)$$

$$\tilde{f}_{i+\frac{1}{2}} = f_{i+\frac{1}{2}}^{Riemann}(\phi_{i+\frac{1}{2}}^L, \phi_{i+\frac{1}{2}}^R). \quad (3)$$

Reconstruction (convection) schemes are required to obtain  $\phi_{i+\frac{1}{2}}^L, \phi_{i+\frac{1}{2}}^R$ .

Godunov's theorem

No linear convection scheme of second-order accuracy or higher can be monotonic.

# Research Background

An ideal non-linear reconstruction scheme:

- 1. High-order accuracy (at least 2nd order) and low-dissipation.
- 2. Oscillation-free across discontinuities.
- 3. Ideally in a compact stencil.
- 4. Scale-invariant, free from case-dependent parameters.

Issues of existing non-linear schemes in a three-cell-based stencil

- ◆ TVD (van Leer, van Albada, MUSCL) and NVD: diffusive and distort shape of transported scalar (smearing, clipping, squaring).
- ◆ WENO3: scale-dependent, low-accuracy (even lower than 2nd order).
- ◆ WENO3+: grid- and case-dependent parameters.
- ◆ Non-polynomial based scheme (LDLR, THINC): singularity, computationally expensive.

There are no schemes in a compact stencil that can achieve high-resolution, scale-invariant and scalar-structure-preserving properties simultaneously.

## Research Aim

- Unify existing schemes into one framework.
- Based on the unified work, design high-resolution, scale-invariant and scalar-structure-preserving schemes.
- Extend the proposed schemes to unstructured grid, and implement into CFD software such as OpenFOAM.
- Simulations of high-speed compressible single and multi-phase flows with the new scheme.

# Contents

## 1 Introduction

- Research Background
- Research Aim

## 2 A Unified Framework for Non-linear Schemes in a Compact Stencil

- Definitions and Properties of the Normalised Variable
- Accuracy Condition
- Review of Existing Non-linear Schemes
- Unified Normalised-variable Diagram

## 3 Reconstruction Operator on Unified Normalised-variable Diagram (ROUND) schemes

## 4 Extension to unstructured girds and implementation into OpenFoam

## 5 Conclusion

# Definitions and Properties of the Normalised Variable

## Definition

With initial VIA in a compact stencil  $S_i = \{I_{i-1}, I_i, I_{i+1}\}$ , left-side-biased Normalised Volume Integrated Average (NVIA) value  $\hat{\phi}_i^L$  over cell  $I_i$  is defined as

$$\hat{\phi}_i^L = \frac{\bar{\phi}_i - \bar{\phi}_{i-1}}{\bar{\phi}_{i+1} - \bar{\phi}_{i-1}}. \quad (4)$$

Left-side-biased Normalised Reconstruction Value (NRV)  $\hat{\phi}_{i+1/2}^L$  at the cell boundary  $x_{i+1/2}$  is defined as

$$\hat{\phi}_{i+1/2}^L = \frac{\phi_{i+1/2}^L - \bar{\phi}_{i-1}}{\bar{\phi}_{i+1} - \bar{\phi}_{i-1}}. \quad (5)$$

## Definition

The smooth function  $\phi(x)$  is said to have a critical point of order  $p_c$  at  $x_c$  if  $\phi'(x_c) = \dots = \phi^{(p_c)}(x_c) = 0$  but  $\phi^{(p_c+1)}(x_c) \neq 0$ .

# Definitions and Properties of the Normalised Variable

## Lemma

Suppose there is no critical point for a smooth function  $\phi(x)$  in  $S_i$ , there is

$$\hat{\phi}_i^L = \frac{1}{2} - \frac{\phi''(x_c)h}{4\phi'(x_c)} + O(h^2), \quad (6)$$

for a point  $x_c = x_{i-1/2} + \delta h$ ,  $-1 \leq \delta \leq 2$ .

## Lemma

Assume that a smooth function  $\phi(x)$  contains a first-order critical point at  $x_c = x_{i-1/2} + \delta h$  in  $S_i$ ,  $\delta \neq 1/2$  and  $-1 \leq \delta \leq 2$ , there is

$$\hat{\phi}_i^L = \frac{\delta}{-1 + 2\delta} + O(h). \quad (7)$$

# Definitions and Properties of the Normalised Variable

## Proposition

Assume that a smooth function contains a first order critical point and the mesh size is fine enough. When the first order critical point is in cell  $I_i$ , there is  $\hat{\phi}_i^L < 0$  or  $\hat{\phi}_i^L > 1.0$ . When the first order critical point is in cell  $I_{i-1}$ , there is  $0 < \hat{\phi}_i^L < \frac{1}{2}$ . When the first order critical point is in cell  $I_{i+1}$ , there is  $\frac{1}{2} < \hat{\phi}_i^L < 1.0$ .

## Definition

Normalised reconstruction operator  $\hat{\mathcal{R}}_i^L$  is defined as a function of NVIA to get NRV as  $\hat{\phi}_{i+1/2}^L = \hat{\mathcal{R}}_i^L[\hat{\phi}_i^L]$ .

## Proposition

A normalisable scheme is scale-invariant.

# Accuracy Condition of Linear $\hat{\mathcal{R}}_i^L$

The corresponding normalised linear reconstruction operator  $\hat{\mathcal{R}}_i^{L,Linear}$  can be written as

$$\hat{\mathcal{R}}_i^{L,Linear} = \alpha_1 \hat{\phi}_i^L + \alpha_0, \quad (8)$$

The truncation error  $E$  can be obtained as

$$E = \left(\frac{3}{2} - \alpha_1 - 2\alpha_0\right)\phi'(x_c)h + \left(\frac{1}{3} - \alpha_0 + \delta\left(-\frac{3}{2} + \alpha_1 + 2\alpha_0\right)\right)\phi''(x_c)h^2 + \dots \quad (9)$$

## Proposition

A sufficient and necessary condition for  $\hat{\mathcal{R}}_i^{L,Linear}$  to achieve at least second-order accuracy is that  $\hat{\mathcal{R}}_i^{L,Linear}$  passes through  $(\frac{1}{2}, \frac{3}{4})$  in the normalised-variable space.

A sufficient and necessary condition for  $\hat{\mathcal{R}}_i^{L,Linear}$  to achieve a uniform third-order accuracy is that  $\alpha_0 = \frac{1}{3}$  and  $\alpha_1 = \frac{5}{6}$ .

# Accuracy Condition of Linear $\hat{\mathcal{R}}_i^L$

## Proposition

For a second-order linear reconstruction operator, numerical diffusion and numerical anti-diffusion errors are dependent on  $\alpha_0$  and  $\hat{\phi}_i^L$ , and are introduced in the following way:

$$\begin{cases} \text{Numerical diffusion} & \text{if } \alpha_0 > \frac{1}{3}, \hat{\phi}_i^L > \frac{1}{2} \text{ or } \alpha_0 < \frac{1}{3}, \hat{\phi}_i^L < \frac{1}{2} \\ \text{Numerical anti-diffusion} & \text{if } \alpha_0 > \frac{1}{3}, \hat{\phi}_i^L < \frac{1}{2} \text{ or } \alpha_0 < \frac{1}{3}, \hat{\phi}_i^L > \frac{1}{2} \end{cases} , \quad (10)$$

# Accuracy Condition of Linear $\hat{\mathcal{R}}_i^L$

Proof.

Assuming the smooth function does not contain any critical points over the targeted compact stencil, Eq.(9) can be reformulated into

$$E^{2nd} = \left(\frac{1}{3} - \alpha_0\right) \frac{\phi''(x_c)}{\phi'(x_c)} \phi'(x_c) h^2 + O(h^3). \quad (11)$$

By truncating Eq.(6) to the first order term and substituting into the above equation, there is

$$E^{2nd} = 4\left(\frac{1}{3} - \alpha_0\right)\left(\frac{1}{2} - \hat{\phi}_i^L\right) \phi'(x_c) h + O(h^3). \quad (12)$$

Note  $\phi'(x_c)$  can be considered a diffusion term. Then, when  $\hat{\phi}_i^L$  and  $\alpha_0$  produce a negative sign of the leading term in Eq.(12), the numerical anti-dissipation is introduced. Otherwise, numerical dissipation is introduced. □

# Accuracy Condition in Unified Normalised-variable Diagram (UND)

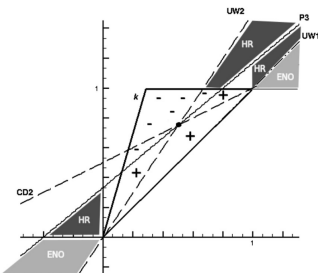


**Figure:** The line of  $\hat{\mathcal{R}}_i^{L,P3}$  is the only linear reconstruction operator that achieves a uniform third-order accuracy. A numerical diffusion region marked with + symbol and a numerical anti-diffusion region marked with -.

How much accuracy can we achieve without causing numerical oscillations?  
How much anti-diffusion can we introduce without distorting the shape of transported scalar?

To answer these questions, we review the existing non-linear schemes using the normalised-variable diagram.

## Review of Existing Non-linear Schemes: TVD

TVD flux limiter:

$$\hat{\mathcal{R}}_i^{L,TVD} = \hat{\phi}_i^L + \frac{1}{2}\psi\left(\frac{\hat{\phi}_i^L}{1 - \hat{\phi}_i^L}\right)(1 - \hat{\phi}_i^L). \quad (13)$$

When TVD flux limiter function satisfies the symmetric condition  $\frac{\psi(r)}{r} = \psi(\frac{1}{r})$ , the symmetric TVD flux limiter can be written into the form of the TVD slope limiter. The reconstruction operator of the TVD slope limiter can also be normalised as

$$\hat{\mathcal{R}}_i^{L,TVD} = \hat{\phi}_i + \frac{1}{4}\tilde{\psi}\left(\frac{1 - \hat{\phi}_i}{\hat{\phi}_i}\right). \quad (14)$$

Some well-known symmetric TVD flux limiters are Minmod, Superbee, van Leer, van Albada, and OSPRE. After some manipulations, the symmetric property of the slope limiter can be expressed as

$$\tilde{\psi}(1 - \hat{\phi}_i^L) = \tilde{\psi}(\hat{\phi}_i^L). \quad (15)$$

# Review of Existing Non-linear Schemes: TVD

The reasons why symmetric TVD have smearing, clipping, and squaring effect:

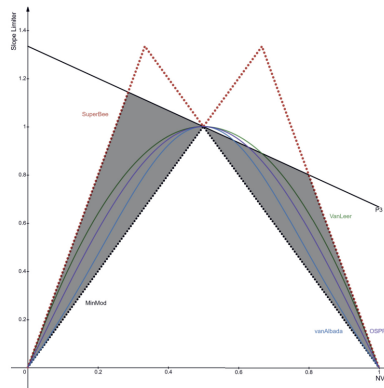
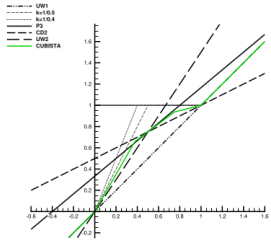
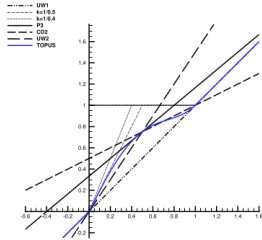


Figure: The diagram of TVD slope limiter with NVIA. The region in grey colour is the numerical dissipation region. (1)The unsymmetrical numerical dissipation of symmetric TVD limiters is likely to distort the shape of the passive transported scalar. (2)Symmetric TVD limiters do not have third-order accuracy.

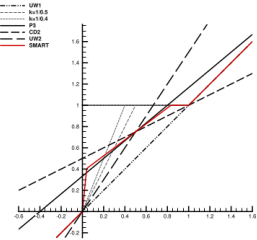
# Review of Existing Non-linear Schemes: NVD



(a) CUBISTA



(b) TOPUS

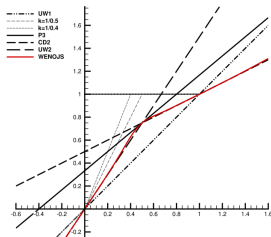


(c) SMART

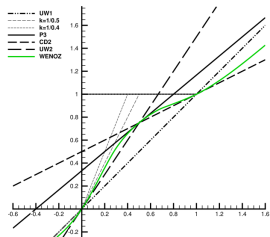
**Figure:** NVD schemes have the same issue as the TVD schemes.

# Review of Existing Non-linear Schemes: WENO

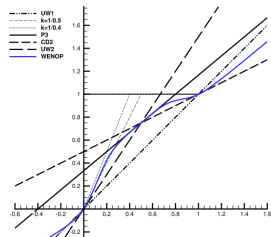
$$\mathcal{R}_i^{L,WENO} = \omega_0 \mathcal{R}_i^{L,UW2} + \omega_1 \mathcal{R}_i^{L,CD2}, \quad (16)$$



(a) WENO-JS



(b) WENO-Z



(c) WENO-P

**Figure:** WENO schemes are scale-dependent and cannot be normalised directly. Thus, we plot WENO reconstruction operators in the normalised-variable space by assigning  $\bar{\phi}_{i-1} = 0$  and  $\bar{\phi}_{i+1} = 1$ .

# Review of Existing Non-linear Schemes: WENO-P+

$$\zeta_k = d_k \left( 1 + \frac{\tau_P}{IS_k + \epsilon} + s \frac{IS_k + \epsilon}{\tau_P + \epsilon} \right), k = 0, 1, \quad (17)$$

where  $s = h^P$  is a grid-size dependent parameter. Thus, WENO-P+ is neither scale-invariant nor mesh-size-independent.

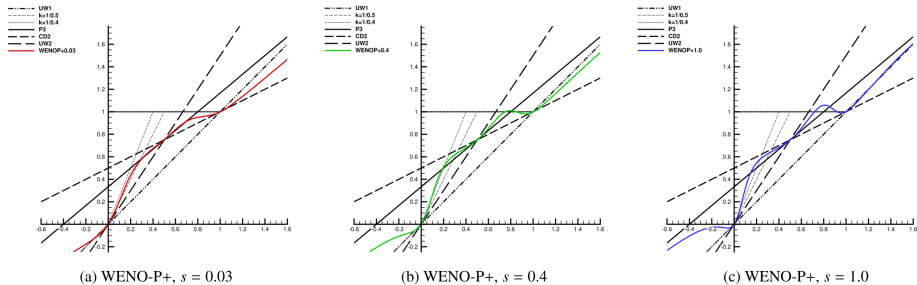


**Figure:** The WENO-P+ reconstruction operator in the normalised-variable space by assigning  $\bar{\phi}_{i-1} = 0$ ,  $\bar{\phi}_{i+1} = 1$  and  $h = \frac{1}{200}$ . The numerical results with different parameters: Xu, W. & Wu, W., 2018. *J. Sci. Comput.*, 75, pp.1808-1841.

# Review of Existing Non-linear Schemes: LDLR

$$\mathcal{P}^{LDLR}(x) = A_1 + A_2 \ln(x - x_i + A_3) + A_4 \ln(x - x_i + A_5), \quad (18)$$

$$\hat{\mathcal{R}}_i^{L, LDLR} = \hat{\phi}_i^L + \frac{2\varphi \left( (\varphi^2 + 1) \cdot (1 - \hat{\phi}_i^L) - 2.0 \cdot \varphi \cdot \hat{\phi}_i^L \right) \cdot \ln \varphi - (1 - 2\hat{\phi}_i^L)(\varphi^2 - 1)}{2(\varphi^2 - 1) \cdot (\varphi - 1)^2}, \quad (19)$$

$$\varphi = 2 \cdot \frac{|\hat{\phi}_i^L|^q - |\hat{\phi}_i^L|^q}{|1 - \hat{\phi}_i^L|^{2q} + |\hat{\phi}_i^L|^{2q}}, \quad (20)$$

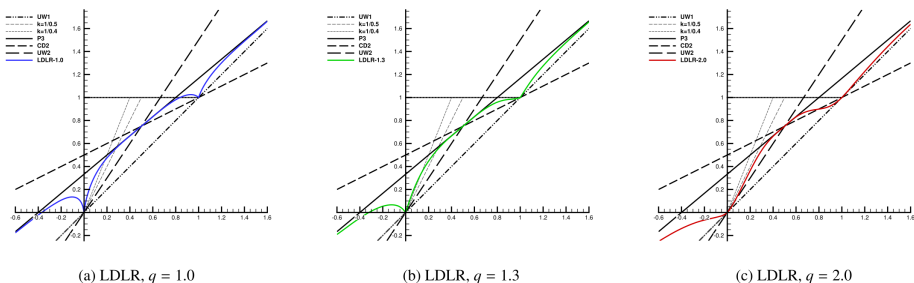
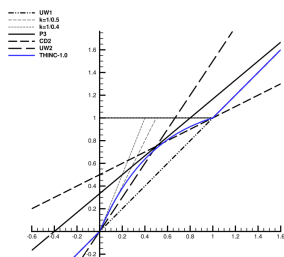


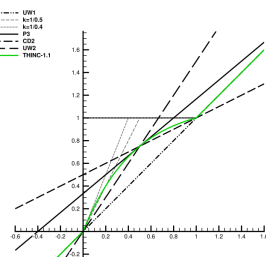
Figure: Diagrams of the normalised LDLR reconstruction operator.

# Review of Existing Non-linear Schemes: THINC

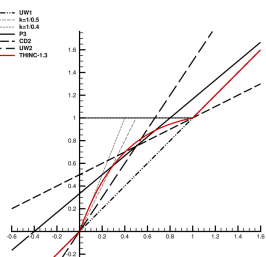
$$\hat{\mathcal{R}}_i^{L, THINC} = \begin{cases} \frac{\sinh(\beta) + \cosh(\beta) - \exp(\beta(-2.0\hat{\phi}_i^L + 1.0))}{2\sinh(\beta)} & 0 < \hat{\phi}_i^L < 1.0 \\ \hat{\phi}_i^L & \text{otherwise} \end{cases} \quad (21)$$



(a) THINC,  $\beta = 1.0$



(b) THINC,  $\beta = 1.1$



(c) THINC,  $\beta = 1.3$

Figure: Diagrams of the normalised THINC reconstruction operator.

# Unified Normalised-variable Diagram

- **CBC-TVD** region: based on TVD schemes.
- **Essentially Non-Oscillatory (ENO)** region: based on WENO and LDLR schemes.
- **High-Resolution (HR)** region: based on WENO-P+ and LDLR.

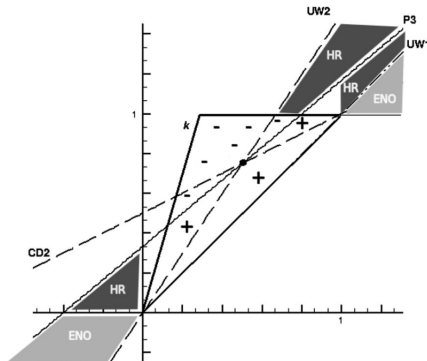


Figure: Unified normalised-variable diagram.

# Contents

## 1 Introduction

- Research Background
- Research Aim

## 2 A Unified Framework for Non-linear Schemes in a Compact Stencil

- Definitions and Properties of the Normalised Variable
- Accuracy Condition
- Review of Existing Non-linear Schemes
- Unified Normalised-variable Diagram

## 3 Reconstruction Operator on Unified Normalised-variable Diagram (ROUND) schemes

## 4 Extension to unstructured girds and implementation into OpenFoam

## 5 Conclusion

# Reconstruction Operator on Unified Normalised-variable Diagram (ROUND) schemes

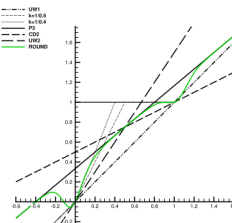
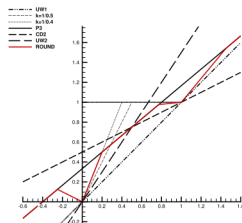
Diffusive ROUND schemes:

Piecewise linear function :

$$\hat{\mathcal{R}}_i^{L,ROUND} = \begin{cases} \min\left(-\frac{1}{2}\hat{\phi}_i^L, \frac{1}{3} + \frac{5}{6}\hat{\phi}_i^L\right) & \text{if } \hat{\phi}_i^L \leq 0.0, \\ \min\left(\min\left(\frac{5}{2}\hat{\phi}_i^L, \frac{1}{3} + \frac{5}{6}\hat{\phi}_i^L\right), \frac{1}{10} + \frac{9}{10}\hat{\phi}_i^L\right) & \text{if } 0.0 < \hat{\phi}_i^L \leq 1.0, \\ \min\left(\frac{6}{5}\hat{\phi}_i^L - \frac{1}{5}, \frac{1}{3} + \frac{5}{6}\hat{\phi}_i^L\right) & \text{otherwise} \end{cases} . \quad (22)$$

Differentiable function using general multi-quadric functions

$$w_0 = \frac{1}{3} + \frac{2}{3} \frac{1}{(1+\gamma(\hat{\phi}_i^L)^{2m})^n} - \frac{1}{3} \frac{1}{(1+\gamma(1-\hat{\phi}_i^L)^{2m})^n}, \quad m, n \in N^*, \gamma > 0. \quad (23)$$



# ROUND schemes

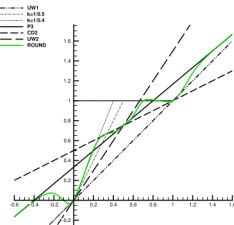
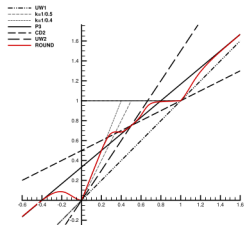
Low-diffusive ROUND schemes:

$$\hat{\mathcal{R}}_i^{L,ROUND} = \left\{ \left[ \frac{1}{3} + \frac{5}{6} \hat{\phi}_i^L + \max(P_0, 0) + \max(P_1, 0) \right] (1 - \omega_0) + \frac{3}{2} \hat{\phi}_i^L \omega_0 \right\} (1 - \omega_1) + \left( \frac{1}{2} \hat{\phi}_i^L + \frac{1}{2} \right) \omega_1, \quad (24)$$

where  $P_0 = 1.1 \times 10^3 (\hat{\phi}_i^L - 0.05)^3 (0.47 - \hat{\phi}_i^L)^3$  and  $P_1 = 1.8 \times 10^4 (\hat{\phi}_i^L - 0.55)^3 (0.97 - \hat{\phi}_i^L)^5$ .

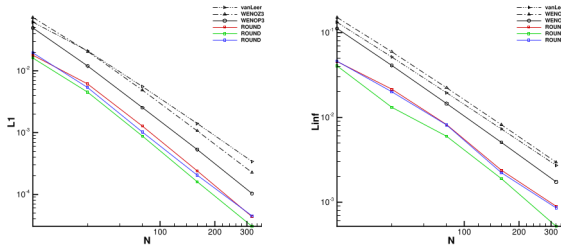
Weighting functions  $\omega_0$  and  $\omega_1$  are given as  $\omega_0 = \frac{1}{(1 + \gamma_0 (\hat{\phi}_i^L)^2)^4}$  and

$$\omega_1 = \frac{1}{(1 + \gamma_1 (\hat{\phi}_i^L - 1)^2)^8} \text{ where } \gamma_0 = 12.0 \text{ and } \gamma_1 = 5.0.$$

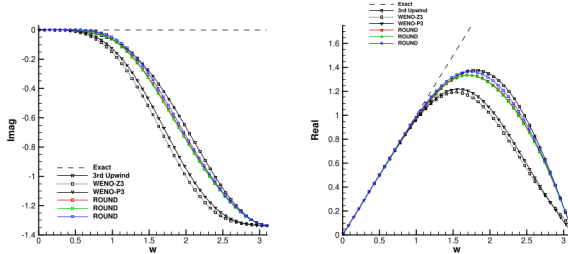


# ROUND schemes: verification and validation

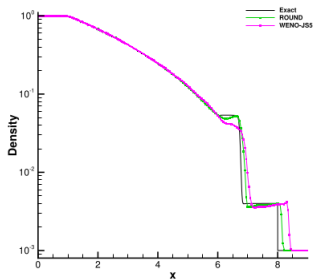
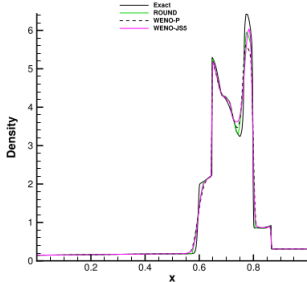
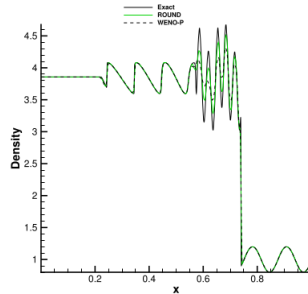
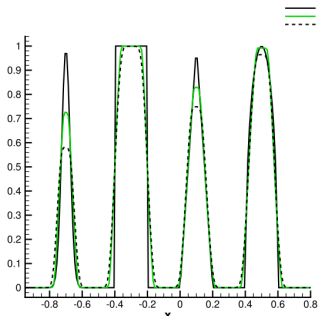
Accuracy tests:



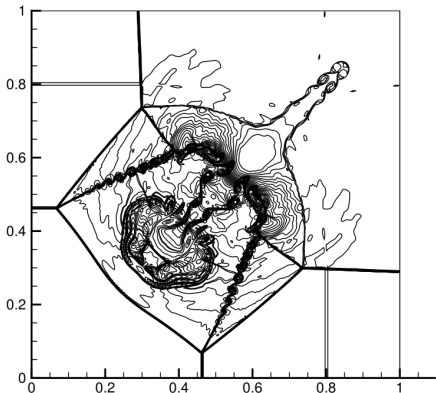
Spectral properties:



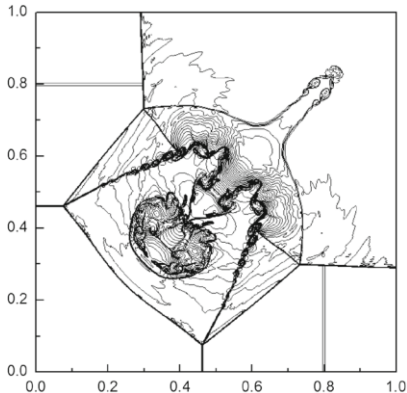
# ROUND schemes: 1D Shock tube



# ROUND schemes: 2D Riemann problem



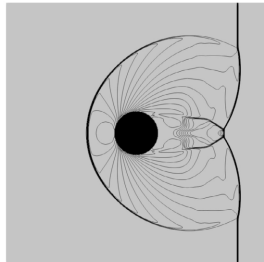
(a) ROUND  $600 \times 600$



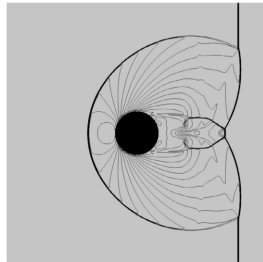
(b) 5th order WENO-Z  $960 \times 960$

**Figure:** 5th order WENO-Z result is produced in W.Xu et. al, *J. Sci. Comput.* 75 (2018) 1808–1841.

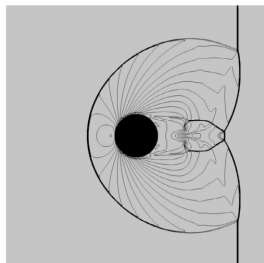
# ROUND schemes: Extension to FDM-IBM



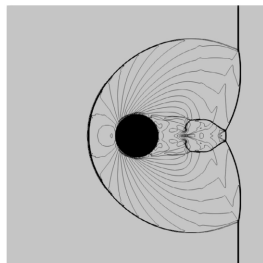
(a) 3rd order WENO-JS



(b) 5th order WENO-JS



(c) Dissipative ROUND



(d) Low-dissipative ROUND

# Contents

## 1 Introduction

- Research Background
- Research Aim

## 2 A Unified Framework for Non-linear Schemes in a Compact Stencil

- Definitions and Properties of the Normalised Variable
- Accuracy Condition
- Review of Existing Non-linear Schemes
- Unified Normalised-variable Diagram

## 3 Reconstruction Operator on Unified Normalised-variable Diagram (ROUND) schemes

## 4 Extension to unstructured grids and implementation into OpenFoam

## 5 Conclusion

# Extension to unstructured girds and implementation into OpenFoam

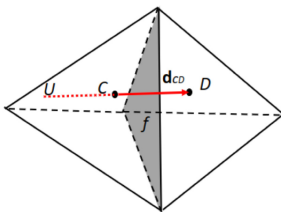


**Figure:** The illustration of two adjacent cells,  $C$  and  $D$ .  $f$  is the cell interface.  $\mathbf{d}_{CD}$  is the vector connecting cell centers  $C$  and  $D$ .  $U$  is the virtual upwind cell point.

The code is released at

<https://github.com/ROUNDschemes/libROUNDSchemes>

# Accuracy test.

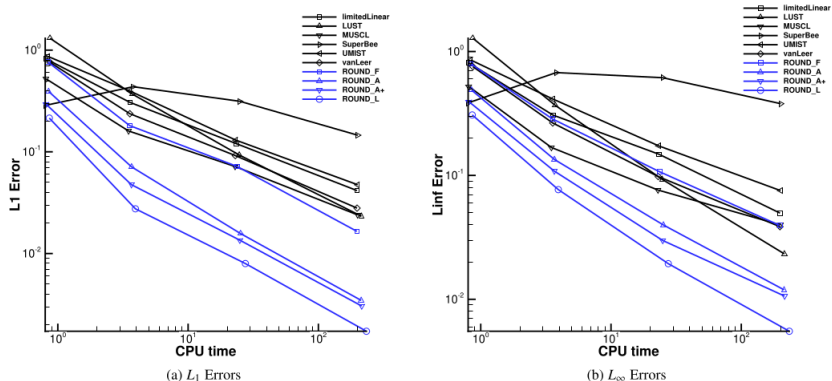
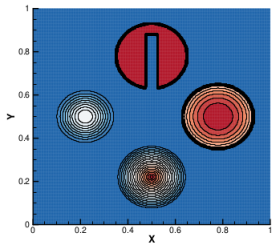


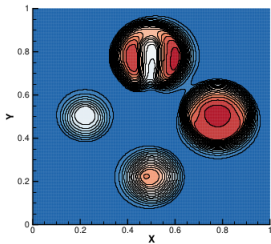
**Figure:** The variation of  $L_1$  errors (a) and  $L_\infty$  errors (b) with mesh size for the accuracy tests.

ROUND schemes significantly reduce numerical errors with similar CPU costs.

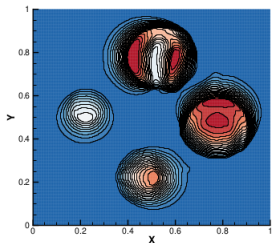
# Convection of complex profiles.



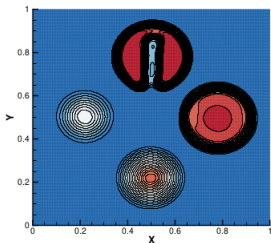
(a) Exact solution



(b) van Leer



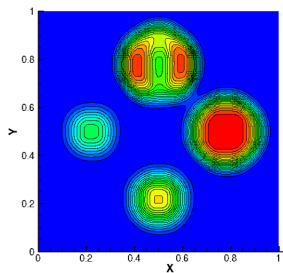
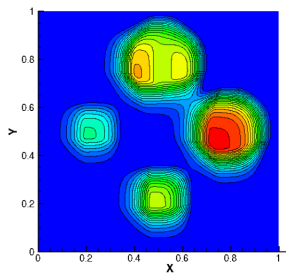
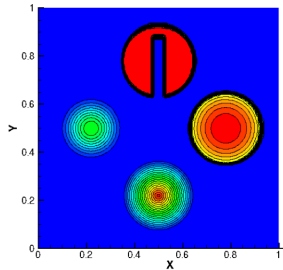
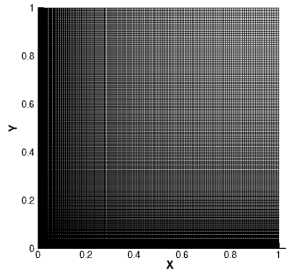
(c) limitedLinear



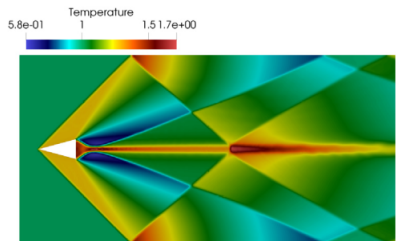
(d) ROUND\_A+

ROUND schemes show high-resolution and scalar-structure-preserving properties.

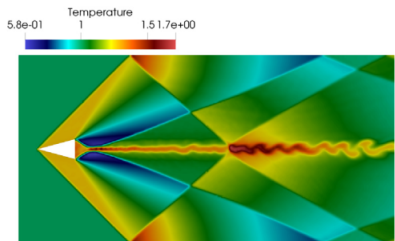
# Convection of complex profiles.



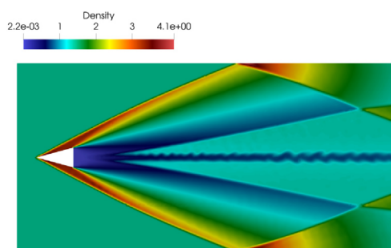
# Supersonic and hypersonic flow over a wedge



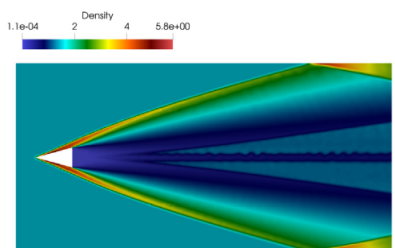
(a) vanLeer



(b) ROUND\_A+

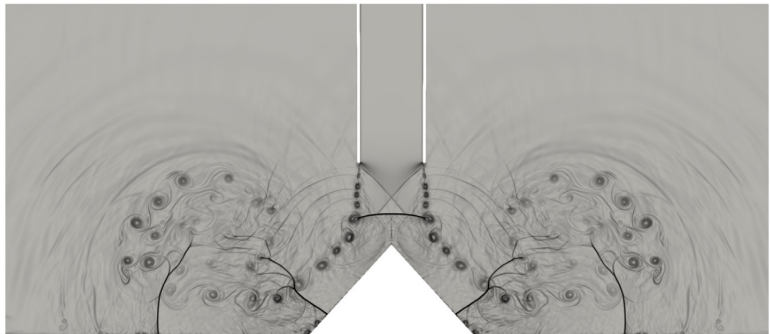


(a) Ma=4

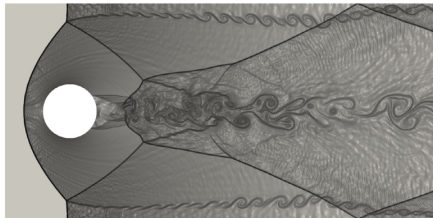


(b) Ma=6

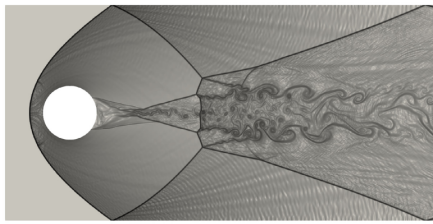
# Impingement of a supersonic jet on a cone mounted on a flat plate



# Supersonic and hypersonic flows around a circular cylinder



(a)  $\text{Ma}=3$



(b)  $\text{Ma}=5$

**Figure:** Numerical results of the magnitude of the density gradient fields for the supersonic and hypersonic flows over a circular cylinder.

# Large-eddy simulation of bluff-body stabilized premixed flames

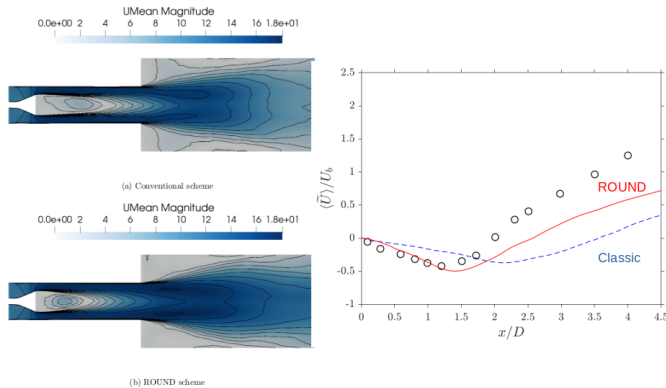


**Figure:** ROUND schemes can better preserve the time-averaged field's statistical axis-symmetry compared with conventional schemes.

# Contents

## 1 Introduction

- Research Background
- Research Aim

## 2 A Unified Framework for Non-linear Schemes in a Compact Stencil

- Definitions and Properties of the Normalised Variable
- Accuracy Condition
- Review of Existing Non-linear Schemes
- Unified Normalised-variable Diagram

## 3 Reconstruction Operator on Unified Normalised-variable Diagram (ROUND) schemes

## 4 Extension to unstructured girds and implementation into OpenFoam

## 5 Conclusion

# Conclusion

## Conclusion

- New efficient schemes named ROUND are proposed based on a unified framework of existing non-linear schemes in a compact stencil.
- The new schemes have **high-resolution, scale-invariant, scalar-structure-preserving** properties.
- ROUND is implemented in OpenFOAM and verified by various problems.

## References

- [1]Deng, X., 2023. "A Unified Framework for Non-linear Reconstruction Schemes in a Compact Stencil. Part 1: Beyond Second Order." *Journal of Computational Physics*, p.112052.
- [2]Deng, X., 2023. "A new open-source library based on novel high-resolution structure-preserving convection schemes." *Journal of Computational Science*, p.102150.
- [3]Deng, X., Massey, J.C. and Swaminathan, N., 2023. "Large-eddy simulation of bluff-body stabilized premixed flames with low-dissipative, structure-preserving convection schemes." *AIP Advances*, 13(5).
- [4]Cheng, L., Deng, X. and Xie, B., 2023. "An accurate and practical numerical solver for simulations of shock, vortices and turbulence interaction problems." *Acta Astronautica*, 210, pp.1-13.
- [5]Deng, X., Jiang, Z.H. and Yan, C., 2024. "Efficient ROUND schemes on non-uniform grids applied to discontinuous Galerkin schemes with Godunov-type finite volume sub-cell limiting." *Journal of Computational Physics*, p.113575.